

SGR 0418+5729 as an evolved Quark-Nova compact remnant

R. Ouyed*, D. Leahy and B. Niebergal

Department of Physics and Astronomy, University of Calgary, 2500 University Drive NW, Calgary, Alberta, T2N 1N4 Canada

Accepted —. Received —; in original form —

ABSTRACT

Soft gamma repeaters and anomalous X-ray pulsars are believed to be magnetars, i.e. neutron stars powered by extreme magnetic fields, $B \sim 10^{14}$ – 10^{15} Gauss. The recent discovery of a soft gamma repeater with low magnetic field ($< 7.5 \times 10^{12}$ Gauss), SGR 0418+5729, which shows bursts similar to those of SGRs, implies that a high surface dipolar magnetic field might not be necessary for magnetar-like activity. We show that the quiescent and bursting properties of SGR 0418+5729 find natural explanations in the context of low-magnetic field Quark-Nova (detonative transition from a neutron star to a quark star) remnants, i.e. an old quark star surrounded by degenerate (iron-rich) Keplerian ring/debris ejected during the Quark-Nova explosion. We find that a 16 Myr old quark star surrounded by a $\sim 10^{-10} M_{\odot}$ ring, extending in radius from ~ 30 km to 60 km, reproduces many observed properties of SGR 0418+5729. The SGR-like burst is caused by magnetic penetration of the inner part of the ring and subsequent accretion. Radiation feedback results in months-long accretion from the ring’s non-degenerate atmosphere which matches well the observed decay phase. We make specific predictions (such as an accretion glitch of $\Delta P/P \sim -2 \times 10^{-11}$ during burst and a sub-keV proton cyclotron line from the ring) that can be tested by sensitive observations.

Key words: stars: neutron : magnetic fields.

1 INTRODUCTION

Soft γ -ray Repeater (SGRs) are sources of recurrent, short ($t \sim 0.1$ s), intense ($L \sim 10^{37-42}$ ergs) bursts of γ -ray emission with an energy spectrum characterized by temperatures of ~ 100 keV. Occasionally SGRs enter into active episodes producing many short X-ray bursts; extremely rarely (about once per 50 years per source), SGRs emit a giant flare, an event with total energy at least 1000 times higher than their typical bursts. The normal pattern of SGRs is intense activity periods which can last weeks or months, separated by quiescent phases lasting years or decades. Current theory explains this energy release as the result of a catastrophic re-configuration of a magnetar’s magnetic field. AXPs are similar in nature but with a somewhat weaker intensity and no recurrent bursting. Several SGRs/AXPs have been found to be X-ray pulsars with unusually high spin-down rates, usually attributed to magnetic braking caused by their super-strong magnetic field. In all sources with magnetar-like activity, the dipolar fields span $5 \times 10^{13} \text{ G} < B < 2 \times 10^{15} \text{ G}$, which is ~ 10 – 1000 times the average value in radio pulsars. Magnetar-like activity previously was observed only in

sources with dipolar magnetic fields stronger than the electron quantum field, $B_Q = m_e^2 c^3 / e \hbar \sim 4.4 \times 10^{13}$ Gauss.

SGR 0418+5729 was discovered on 5 June 2009 when the Fermi Gamma-ray Burst Monitor (GBM) observed two magnetar-like bursts (van der Horst et al. (2010)). Follow-up observations with several x-ray satellites show that it has x-ray pulsations at ~ 9.1 s, well within the range of periods of SGR sources (Gögüş et al. (2009); Esposito et al. (2010)). The implied upper limit on the period derivative of SGR 0418+5729 of $\dot{P} < 6.0 \times 10^{-15} \beta$ is by far the smallest of all known SGRs/AXPs. The corresponding limit on the surface dipolar magnetic field of SGR 0418+5729 is $B < 7.5 \times 10^{12}$ Gauss, making it the SGR with the lowest surface dipolar magnetic field yet. The upper limit on the period derivative implies a characteristic age of the source in excess of > 24 Myr in the standard dipole model, $P/(2\dot{P})$. Despite such a low surface magnetic field ($\ll B_Q$), SGR 0418+5729 exhibits all the typical characteristics of an SGR. Its bursting properties can be summarized as follows (van der Horst et al. (2010); Gögüş et al. (2009); Esposito et al. (2010)):

- At a distance of 2 kpc, assuming that the source is located in the Perseus arm, the estimate energies of the two

* E-mail: rouyed@ucalgary.ca (RO)

observed bursts (in the 8-200 keV range) are 4×10^{37} erg and 2×10^{37} erg, which is at the lower end of the distribution compared to other SGR bursts but at the high end for AXP ones.

- An optically-thin thermal bremsstrahlung provides the best fit in both bursts (see Table 2 in van der Horst et al. (2010)). The spectrum softens from $kT \sim 33$ keV in the first burst to $kT \sim 20$ keV in the second burst in the time period of ~ 20 minutes which separated the two bursts.

- Immediately following the burst and for the first 160 days (before it disappeared behind the sun), SGR 0418+5729 flux declined by an order of magnitude from $\sim 3 \times 10^{-11}$ erg cm $^{-2}$ s $^{-1}$ ($L_X \sim 1.4 \times 10^{34}$ erg s $^{-1}$) to $\sim 3 \times 10^{-12}$ erg cm $^{-2}$ s $^{-1}$ ($L_X \sim 1.4 \times 10^{33}$ erg s $^{-1}$). The corresponding blackbody temperature declined from 1 keV to 0.8 keV (see Figure 2 in Esposito et al. (2010)).

- The burst luminosity is $\sim 10^{39}$ erg s $^{-1}$ with burst temperature in the 20-30 keV range. Assuming blackbody emission the emitting area can be estimated to be on average $A_b \sim 8.5 \times 10^8$ cm 2 .

SGR 0418+5729's current properties (i.e. following the bursting era) show a spectrum which is well fit by an absorbed blackbody with a line-of-sight absorption $N_H = (1.5 \pm 1.0) \times 10^{21}$ cm $^{-2}$ and $kT = 0.67 \pm 0.11$ keV. Using the current luminosity of 6×10^{31} erg s $^{-1}$, and a blackbody temperature of 0.67 keV (Rea et al. (2010)) the emitting area is $A_q \sim 3.1 \times 10^8$ cm 2 ($\ll 4\pi(10 \text{ km})^2$) indicative of a hot spot on the surface of the star.

Since the internal field strength required to produce crustal cracking in the Magnetar model should be typically in excess of 10^{14} Gauss (Thompson & Duncan (1995)), one wonders how SGR 0418+5729, with its weak surface magnetic field, can harbor a much stronger magnetic field in its crust. In fact, for such an old source (> 24 Myr) it would take an even stronger internal field to crack the cold crust¹. Could such a difference between the surface and crustal field be possible and sustainable? What mechanism could lead to such a gradient, and if it exists does it mean that some ordinary pulsars are dormant SGRs waiting to erupt? Maybe a strong magnetic field is not necessary to explain SGR behavior. The existence of radio pulsars with $B > B_Q$ and, so far, showing only normal behavior (Kaspi (2010)) is another clue that magnetic fields larger than the quantum electron field alone may not be a sufficient condition for the onset of magnetar-like activity.

Here we present an alternative model which offers natural answers to these outstanding questions. In our model high magnetic field strength is not necessary to explain the bursting phase of SGRs and AXPs: It involves an aligned rotator (a quark star; hereafter QS) and iron-rich debris material in the close vicinity (~ 20 -100 km) of the QS star. The QS is the compact remnant of the Quark-Nova (QN) explosion, a detonative transition from a neutron star (NS) to a QS (Ouyed et al. (2002); Vogt et al. (2004); Niebergal et al.

(2010b)). The QN detonation also leads to ejection of the NS outer layers (Keränen et al. (2005)). If the QS is born slowly rotating, then the debris formed from the QN ejecta will be in co-rotation with the star's dipole field (Ouyed et al. (2007a), hereafter OLN1). Sources born with faster rotation will confine the debris into a Keplerian ring at 20-100 km away from the star (Ouyed et al. (2007b), hereafter OLN2). In our model SGRs are QS with a co-rotating shell while AXPs are QS with a Keplerian ring. The debris consists of $\sim 10^{-6} M_\odot$ of iron-rich degenerate material. The initial QS surface magnetic field is 10^{15} G. Such initial extreme surface magnetic fields are natural values for quark stars experiencing color ferromagnetism before they enter the color superconducting phase (Iwazaki (2005)).

The paper is organized as follows. Section 2 is a summary of our previous works and sets the stage for this work. Section 3 is the application of our model to evolved accreting QS-ring systems. The thermal feedback between the QS and the ring depends critically on the ring geometry, which evolves from thick to thin. For old sources, the resulting behavior is in a different regime than considered in previous papers. This leads to new forms of the equations, which we then fit to the observations. We conclude in Section 4.

2 SGRS AND AXPS IN OUR MODEL

2.1 The aligned rotator and the vortex band

The QS is born an aligned rotator since the superconducting QS confines the interior magnetic field to vortices aligned with the rotation axis³ (Ouyed et al. (2004, 2006)). As the star spins down via EM emission, vortices (and their confined magnetic field) are expelled, leading to magnetic field reconnection at the surface of the star. The period and magnetic field during spin-down evolve as (Niebergal et al. (2006)) $B = B_0(1 + \frac{t}{\tau_0})^{1/6}$ and $P = P_0(1 + \frac{t}{\tau_0})^{1/3}$. Here $\tau_0 = 840 \text{ s } P_{0,\text{ms}}^2 / B_{0,15}^2$ with birth period and magnetic field in millisecond and 10^{15} G, respectively. The period derivative is $\dot{P} = \dot{P}_0(1 + \frac{t}{\tau_0})^{-2/3}$ with $\dot{P}_0 = P_0 / (3\tau_0)$ and characteristic age $t_{\text{age}} = P / 3\dot{P}$ different from $t_{\text{age}} = P / 2\dot{P}$ in the standard dipole model because vortex expulsion changes the magnetic braking index from $n = 3$ (the theoretical value for an aligned spinning dipole) to $n = 4$. This gives $t_{\text{age}} > 16$ Myr for SGR 0418+5729. After 16 Myr of spin-down, the initial magnetic field $\sim 10^{15}$ G will be reduced to $\sim 10^{13}$ G.

Vortex expulsion leads to an X-ray luminosity given by $L_{X,v} \sim 2 \times 10^{35}$ erg s $^{-1} \eta_X \dot{P}_{-11}^2$ where the subscript "v" stands for vortex and η_X is an efficiency parameter (see OLN1 and Ouyed et al. (2006)); \dot{P} is in units of 10^{-11} s s $^{-1}$. Shown in Figure 2 is the L_X - \dot{P} diagram with the vortex band shown (Ouyed et al. (2006); OLN1).

¹ However there are no observational constraints on multipole moments of the surface field or on the internal toroidal magnetic field to rule out the crust cracking model. The tearing mode instability model proposed for magnetic field decay could account for short timescale bursts (< 1 yr) if the dissipation scale is much shorter than typical crust scale ($\ll 10^4$ cm) (Lyutikov (2003)).

² This ring is unlike a fall-back disk around a neutron star (e.g. Trümper et al. (2010)). The ring is iron-rich, very close to the star and degenerate. Similar ring formation when a neutron star is born appears implausible since the proto-neutron star is too large. Later on, there is no mechanism to eject degenerate material unless a violent change of state, like a QN occurs.

³ The aligned magnetic field of the QS provides a natural explanation for the lack of persistent radio pulsation (Ouyed et al. (2004, 2006)).

QS-shell and non-accreting QS-ring systems evolve along the vortex band. QS-ring systems (AXPs) enter an accretion era where their steady X-ray luminosity is dominated by accretion (OLNII). These systems will evolve along the accretion band (see Figure 1), and return to the vortex band (a vortex-dominated phase) much later once the ring is consumed (Ouyed et al. (2009), hereafter OLNIII). In OLNIII RRATs are explained as the result of AXPs descending back to the vortex band.

2.2 Transient AXPs in our model

The QS-Ring system for AXPs allows us to differentiate between AXPs and transient AXPs. Transients AXPs are QS-Ring systems which have not yet entered the accretion-dominated phase and are in the vortex band (Ouyed et al. (2010), hereafter OLNIV). Transient AXPs burst only when the inner wall of the ring is permeated by the magnetic field and is accreted. Only during bursting phase does the ring accrete (OLNIV). During quiescence, these are much quieter than SGRs (although in similar region in the vortex band) since the ring is more stable than the co-rotating shell (OLNI&OLNII).

All of QS-Ring systems should eventually enter an accretion-dominated phase. The onset of accretion is dictated by an interplay between the magnetic field and the ring/atmosphere: The highly conducting degenerate ring is not penetrated by the magnetic field. In OLNIV a “squashed” field was necessary to explain some aspects of transient AXPs, while in OLNII a “stretched” configuration (shown in Figure 1 here) was appropriate. This suggests one evolves into the other as a consequence of ring viscous spreading and magnetic field decay.

2.3 Bursting

The bursting properties of SGRs and AXPs are caused by the interaction between the QN debris material and the star’s magnetic field. This leads to accretion of debris onto the QS. The fundamental difference between the co-rotating shell (SGRs) and the keplerian ring (AXPs) is stability. The co-rotating shell is a very unstable configuration with the shell’s boundary hovering around the magnetic neutrality line prompting more instabilities (and thus more recurrent bursts). The Keplerian ring is more stable and is only perturbed after magnetic field penetration of its inner edge, which triggers the accretion of a small inner part of the ring (i.e. the wall). High magnetic field strength is not a requirement in our model: Wall penetration can occur even in old sources. Below, the quiescent and bursting properties of SGR 0418+5729 are explained in the context of an old evolved accreting QS-ring system.

2.4 Emission components

QS-shell systems (SGRs) and non-accreting QS-ring systems (transient AXPs) in quiescence consist of two emitting components (QS vortex annihilation and shell/ring reprocessing the QS flux). Accreting QS-ring systems (AXPs), during quiescence, have three components: The accreting hot spot, the QS vortex annihilation and the illuminated ring. All types

of systems would burst when chunks of the shell/ring are accreted onto the star. Only during the bursting phase would transient AXPs resemble AXPs (OLNIV).

3 SGR 0418+5729 AS AN EVOLVED ACCRETING QS-RING SYSTEM

Here we describe the properties of an accreting QS-ring system in the case where the system has evolved to low-mass, low-density and different ring geometry. In this section, equations from our previous studies are embedded in the text or un-numbered; while new equations are numbered.

3.1 Ring properties

Figure 1 shows the magnetic field configuration and ring geometry for an old accreting QS-ring system such as SGR 0418+5729. The ring properties are described in detail in §2.2 of OLNIV. Hereafter, subscripts “in” and “out” refer to the inner and outer edge of the ring, respectively. The ring vertical height at a radius R is $H_{\text{ring}} = 2.68 \text{ km} \rho_{\text{ring},9}^{1/6} R_{15}^{3/2}$ where the ring density is in units of 10^9 g cm^{-3} . The ring radial extent, which defines the ring’s outer radius R_{out} in our model, increases by viscous spreading in time as $R_{\text{out}} \simeq \Delta R_{\text{ring}} \sim 7.8 \text{ km} T_{\text{keV}}^{5/4} t_{\text{yrs}}^{1/2}$ with the ring’s temperature and the system’s age in units of keV and years, respectively. The ring average density can be found from $\rho_{\text{ring}} = m_{\text{ring}} / (2\pi R_{\text{out}}^2 H_{\text{ring},\text{out}})$ which gives $\rho_{\text{ring}} \simeq 8 \times 10^7 \text{ gm cm}^{-3} m_{\text{ring},-7}^{6/7} / R_{\text{out},15}^3$; here $m_{\text{ring},-7}$ is the ring’s mass at any given time in units of $10^{-7} M_{\odot}$ (the ring’s initial mass is defined as m_{ring}^0). The characteristics of the ring’s atmosphere are given in §2.3 in OLNIV. The density in the atmosphere is $\rho_{\text{atm.}} = 460 \text{ gm } T_{\text{keV}}^{3/2}$, its height $H_{\text{atm.,in}} = 67.3 \text{ cm } T_{\text{keV}} R_{\text{in},15}^{3/2} / \mu$ with R_{in} expressed in units of 15 km; μ is the mean molecular weight of the ring’s atmosphere. This implies a total mass in the atmosphere of $m_{\text{atm.}} \simeq 2\pi \Delta R_{\text{ring}}^2 \times H_{\text{atm.}} \times \rho_{\text{atm.}} \sim 10^{17} \text{ g } R_{15}^{3/2} T_{\text{keV}}^5 t_{\text{yrs}} / \mu$. The sound speed in the atmosphere is $v_{\text{therm.}} \simeq 1.7 \times 10^7 \text{ cm s}^{-1} T_{\text{keV}}^{1/2} / \mu^{1/2}$.

Inclusion of the T -dependence of the mean molecular weight is a new feature not considered previously. Since the atmosphere is rich in iron-group elements, we can write the mean molecular weight $\mu = 56 / (N_e + 1)$ where N_e is the mean charge of iron given below in three temperatures regimes as measured in experiments (e.g. Arnaud & Rothenflug (1985); see also Kallman & McCray (1982) and Makishima (1986)):

$$\begin{aligned} (N_e + 1) &\sim 9.2 \left(\frac{T}{0.1 \text{ keV}} \right)^{1/4} && \text{for } T < 0.08 \text{ keV} && (1) \\ (N_e + 1) &\sim 10.3 \left(\frac{T}{0.1 \text{ keV}} \right)^{2/3} && \text{for } 0.08 \text{ keV} \leq T \leq 0.4 \text{ keV} \\ (N_e + 1) &\sim 27 && \text{for } T > 0.4 \text{ keV} . \end{aligned}$$

3.2 Quiescent Phase: The accretion Band

The ring leaks out (i.e. accretes) steadily from its atmosphere at the inner radius (see Figure 1), R_{in} , at a rate $\dot{m} = \rho_{\text{atm.}} v_{\text{therm.}} 2\pi R_{\text{in}} (2H_{\text{atm.,in}})$ and accretes onto the surface of the QS creating a hot spot (HS). We get

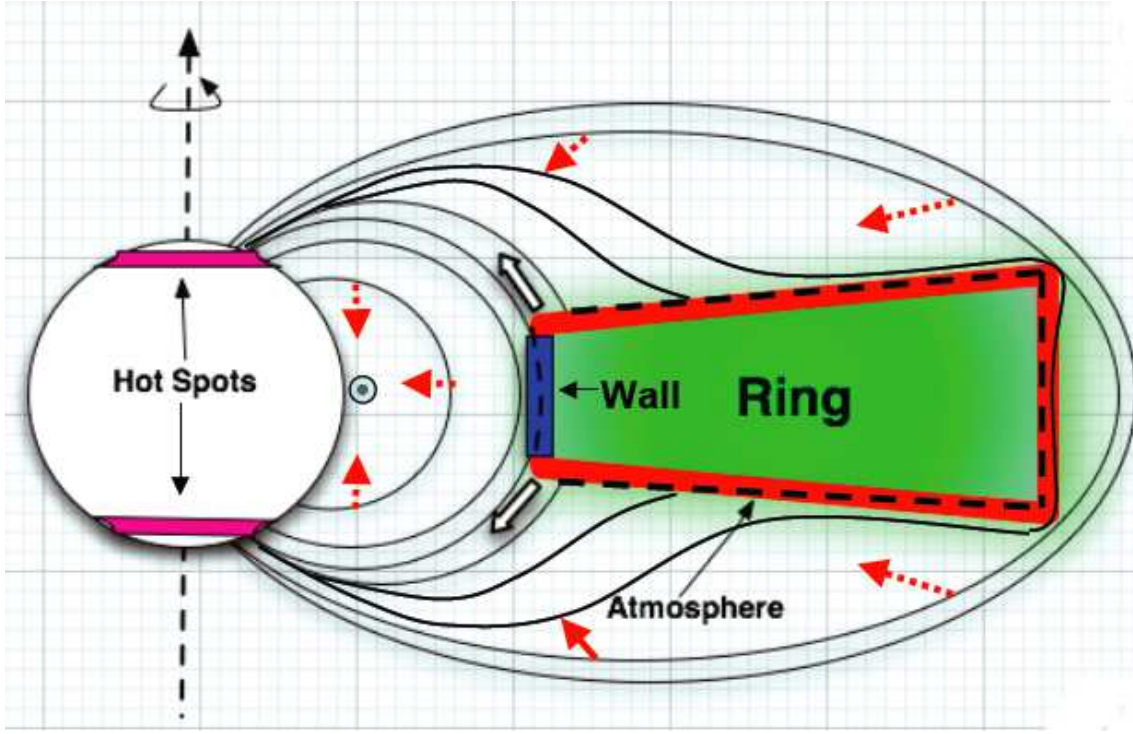


Figure 1. The magnetic field geometry for an old (i.e. $H_{\text{ring}} \ll \Delta R_{\text{ring}}$) QS-ring source; the ring extends from ~ 15 to ~ 100 km radially. The aligned dipole, shrinks inwards (dotted red arrows) as the magnetic field dissipates at the star's equator, and is also stretched by the outward viscous spreading of the ring. Unlike the highly conducting degenerate part of the ring, the non-degenerate atmosphere is quickly penetrated (on timescales of \sim years) by the magnetic field (dashed line) and forced to co-rotate. Accretion (leakage) of the ring's atmosphere ensues at R_{in} as depicted by the white arrows. The emission from the corresponding hot spots (grey bands) yields the quiescent phase emission in our model. The magnetic field penetration of the inner wall occurs every 100 to 1000 years (depending on the system's age) and leads to the bursting phase in our model.

$$\dot{m} \simeq 3.2 \times 10^{17} \text{ g s}^{-1} \frac{T_{\text{keV}}^3 R_{\text{in},15}^{5/2}}{\mu_{q,10}^{3/2}}. \quad (2)$$

Irradiation of the ring by the HS luminosity ($L_{\text{HS}} = \eta \dot{m} c^2$) leads to a feedback mechanism that allows us to estimate the equilibrium temperature of the ring from $\Omega_{\text{ring}} L_{\text{HS}} = A_{\text{ring}} \sigma T_{\text{ring}}^4$ where A_{ring} is the total area of the ring; the irradiation solid angle is Ω_{ring} and depends on the disk geometry and the location of the HS on the surface of the star. We take it as a free parameter (we expect $\Omega_{\text{ring}} < H_{\text{ring}}/R \sim 0.1 m_{\text{ring},-7}^{1/7} (R/R_{\text{out}})^{1/2}$). The ring's equilibrium temperature is then

$$\mu_{q,10}^{3/7} T_{\text{ring}} \sim 3.4 \times 10^{-2} \text{ keV} \frac{\eta_{0.1}^{2/7} R_{\text{in},15}^{5/7} \Omega_{\text{ring}}^{2/7}}{t_{\text{Myr}}^{2/7}}, \quad (3)$$

where $\mu_{q,10} = \mu_{q,10}(T_{\text{ring}})$ is the quiescent mean molecular weight in units of 10; and time is given in units of million years. Replacing the equilibrium temperature in the accretion equation above gives the equilibrium accretion rate

$$\dot{m}_q \sim 1.3 \times 10^{13} \text{ g s}^{-1} \frac{\eta_{0.1}^{6/7} R_{\text{in},15}^{65/14} \Omega_{\text{ring}}^{6/7}}{\mu_{q,10}^{39/14} t_{\text{Myr}}^{6/7}}. \quad (4)$$

The consumption of the ring is thus given as $dm_{\text{ring}}/dt = -\dot{m}_q$ which gives

$$m_{\text{ring}} = m_{\text{ring}}^0 \left(1 - \left(\frac{t}{\tau_{\text{ring}}} \right)^{1/7} \right). \quad (5)$$

with the ring's lifetime

$$\tau_{\text{ring}} \sim 10^5 \text{ yrs} \frac{m_{\text{ring},-6}^0 \mu_{q,10}^{39/2}}{\eta_{0.1}^6 R_{\text{in},15}^{65/2} \Omega_{\text{ring}}^6}. \quad (6)$$

The ring's mass at birth m_{ring}^0 is given in units of $10^{-6} M_{\odot}$. The condition $\tau_{\text{ring}} > t_{\text{age}}$ puts a constraint on the ring's mass at birth, m_{ring}^0 where t_{age} is the system's age.

The corresponding steady accretion luminosity (defining the quiescent phase in our model), $\eta \dot{m}_q c^2$, is

$$L_{\text{HS},q} \sim 1.2 \times 10^{33} \text{ erg s}^{-1} \frac{\eta_{0.1}^{13/7} R_{\text{in},15}^{65/14} \Omega_{\text{ring}}^{6/7}}{\mu_{q,10}^{39/14} t_{\text{Myr}}^{6/7}}, \quad (7)$$

The above equation can be recast into an $L_{\text{HS}} - \dot{P}$ form by recalling that in our model, $\dot{P} = \dot{P}_0 (1 + t/\tau_0)^{-2/3} \sim \dot{P}_0 (t/\tau_0)^{-2/3}$ with $\dot{P}_0 = P_0/(3\tau_0)$. We find

$$L_{\text{HS},q} \sim 1.6 \times 10^{36} \text{ erg s}^{-1} \frac{\eta_{0.1}^{13/7} R_{\text{in},15}^{65/14} \Omega_{\text{ring}}^{6/7}}{\mu_{q,10}^{39/14} (P_{0,\text{ms}} B_{0,15}^2)^{3/7}} \times \dot{P}_{-11}^{9/7}. \quad (8)$$

Shown in Figure 2 is the accretion Band for two cases of $R_{\text{in}} = 12$ km (limited by the QS radius) and $R_{\text{in}} = 40$ km (based on fits from previous work). The region between the accretion band and the vortex band is a "drop" region in our model and defines a regime where the ring becomes fully non-degenerate entering a RRAT phase (OLNIII). It takes millions of years for the ring to become fully non-degenerate,

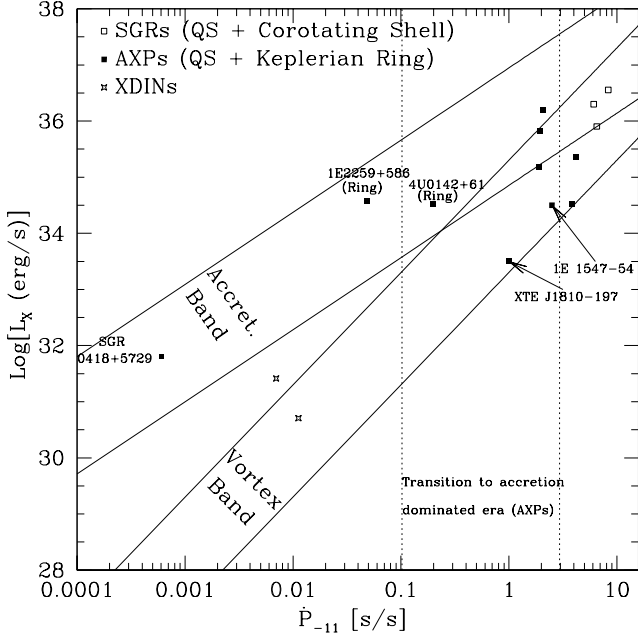


Figure 2. The quiescent phase of SGRs, AXP and XDINs in our model: QS-shell systems (i.e. SGRs) evolve along the vortex band, given by magnetic dissipation at the surface of the star following vortex expulsion and reconnection. Accreting QS-ring systems (i.e. AXP) evolve along the accretion band given by emission from the hot spot (see Figure 1). Transient AXP (XTE J1810–197 and 1E1547–54) are QS-ring systems which have not yet entered the accretion phase and evolve along the vortex band. Old accreting QS-ring systems eventually re-enter the vortex band once they consume their ring. Both QS-shell and QS-ring systems eventually end up at the bottom of the vortex band where XDINs are located.

drastically reducing its accretion rate in the process so that $L_{\text{HS}} < L_v$. RRATs in our model are ring-systems dropping back to the vortex band joining the old shell-less and ring-less systems which are XDINs in our model (see §8 in OLNII).

The HS area on the star area can be estimated from eq.(C1) in OLNIV as $A_{\text{HS}} \simeq 4\pi R_{\text{QS}}^2 (\cos \beta_{\text{max}} - \cos \beta_{\text{in}})$ with

$$\begin{aligned} \sin \beta_{\text{in}} &= \left(\frac{R_{\text{QS}}/R_{\text{in}}}{1 + (H_{\text{ring,in}}/R_{\text{in}})^2} \right)^{1/2} \\ \sin \beta_{\text{max}} &= \left(\frac{R_{\text{QS}}/R_{\text{in}}}{1 + (H_{\text{max}}/R_{\text{in}})^2} \right)^{1/2} \\ H_{\text{max}} &= H_{\text{ring,in}} + H_{\text{atm.,in}} \end{aligned} \quad (9)$$

Since $H_{\text{atm.}} \ll H_{\text{ring}}$, the above becomes

$$A_{\text{HS}} \sim 10^8 \text{ cm}^2 \frac{R_{\text{QS},10}^3}{(1 - \frac{R_{\text{QS}}}{R_{\text{in}}})^{1/2}} \frac{m_{\text{ring},-7}^{1/7}}{\mu_{\text{q},10} T_{\text{keV}}^{1/4} t_{\text{Myr}}^{1/4}} \quad (10)$$

3.3 Bursting phase

3.3.1 Ring penetration and wall accretion

The inner ring is subject to tidal forces which breaks it into vertical “walls” of thickness $\delta r_w = 400 \text{ cm } R_{\text{in},15}^{3/2}$ (eq. 5 in OLNII). The mass of the innermost wall is then $m_w =$

$2\pi R_{\text{in}} \times (2H_{\text{ring,in}}) \times \delta r_w \times \rho_{\text{ring}}$. Including the dependence of ρ_{ring} on other parameters we find,

$$m_w = 7.5 \times 10^{-14} M_{\odot} \frac{m_{\text{ring},-7}^{6/7} R_{\text{in},15}^{7/8} \mu_{\text{q},10}^{15/8}}{\eta_{0.1}^{5/4} t_{\text{Myr}}^{1/2}} \quad (11)$$

The bursting phase is initiated when the innermost wall of the Keplerian ring is magnetically permeated, and forced to co-rotate with the dipolar field, such that it detaches from the ring and is accreted. The corresponding burst energy (the first burst component), $E_b = \eta m_w c^2$, is then

$$E_b \sim 1.3 \times 10^{40} \text{ erg} \frac{m_{\text{ring},-7}^{6/7} R_{\text{in},15}^{7/8} \mu_{\text{q},10}^{15/8}}{\eta_{0.1}^{1/4} t_{\text{Myr}}^{1/2}} \quad (12)$$

In reality, the penetrated wall cracks and breaks into chunks which are then stochastically accreted. The wall is consumed on timescales given by eq.(22) in OLNII which yields a wall consumption time of a few hours. This first component of the bursting phase will be defined by sporadic “spikes”.

3.3.2 Ring irradiation

The second component during the bursting phase consists of the Keplerian ring being irradiated by MeV photons from the accreted wall. The radiation energy hitting the ring is $\Omega_{\text{ring}} E_b$ which leads to photo-disintegration of iron nuclei. To knock-off a proton from iron takes 10.3 MeV, for an α it takes 7.6 MeV and all the way down to Aluminum, it takes 26.9 MeV. So photo-disintegration of iron nuclei enriches the atmosphere with light elements with an average $A \sim 28$. This results in the decrease of the molecular weight, μ , of the ring’s atmosphere from μ_{q} to μ_{b} where subscript “b” stands for burst. The resulting molecular weight is $\mu_{\text{b}} \sim 1$ for a proton-rich atmosphere and $\mu_{\text{b}} \sim 2.1$ for an atmosphere with any other products of γ -disintegration except protons; we adopt an average $\mu_{\text{b}} \sim 1.5$.

The maximum amount in mass of iron disintegrated is $m_{\text{d,max}} = A_{\text{ring}} \rho 2\lambda_{\gamma} = 4\pi R_{\text{out}}^2 \rho \lambda_{\gamma}$ where A_{ring} is the ring’s total area and $\lambda_{\gamma} = 1/(n\sigma_{\text{Fe}})$ is the photon penetration depth with the disintegration cross-section of iron nuclei for 10 MeV photons is of the order of 10^{-25} cm^2 (e.g. Rengarajan (1973)). The density cancels out and we get

$$\begin{aligned} m_{\text{d,max}} &\sim 2.5 \times 10^{27} \text{ g} \frac{T_{\text{keV}}^{5/2} \mu_{\text{q},10} t_{\text{Myr}}}{\sigma_{\text{Fe},-25}} \\ &\sim 4.1 \times 10^{23} \text{ g} \frac{\eta_{0.1}^{5/7} \Omega_{\text{ring}}^{5/7} R_{\text{in},15}^{25/14} t_{\text{Myr}}^{2/7}}{\mu_{\text{q},10}^{1/14} \sigma_{\text{Fe},-25}} \end{aligned} \quad (13)$$

where we made use of equation (3). In reality, the mass of disintegrated iron is limited by the burst energy: $m_{\text{d}} \sim (\Omega_{\text{ring}} E_b / 10 \text{ MeV}) \times 56 m_{\text{H}}$ which gives

$$m_{\text{d}} \sim 1.3 \times 10^{23} \text{ g} \frac{\Omega_{\text{ring}} m_{\text{ring},-7}^{6/7} R_{\text{in},15}^{7/8} \mu_{\text{q},10}^{15/8}}{\eta_{0.1}^{1/4} t_{\text{Myr}}^{1/2}} \quad (14)$$

The atmosphere of the ring evolves back to μ_{q} as (see eq. (27) in OLNII)

$$\frac{1}{\mu(t)} = \frac{1}{\mu_{\text{q}}} + \left(\frac{1}{\mu_{\text{b}}} - \frac{1}{\mu_{\text{q}}} \right) \exp\left(-\frac{t}{\tau_{\text{d}}}\right),$$

where the t_{b} means time since the start of burst, during

which t_{Myr} is constant ($t_b \ll t_{\text{Myr}}$). The corresponding HS luminosity⁴ is

$$L_{\text{HS,b}} = L_{\text{HS,q}} \left(1 + (\mu_r - 1) \exp\left(-\frac{t_b}{\tau_d}\right) \right)^{39/14}, \quad (15)$$

where $\mu_r = \mu_q/\mu_b$ and $\tau_d = m_d/\dot{m}_b$ is the time it takes the irradiated ring to deplete its light-element-rich atmosphere (through accretion at R_{in}). Here \dot{m}_b is given by eq.(4) for $\mu = \mu_b$. This yields

$$\tau_d \sim 189 \text{ days} \frac{\Omega_{\text{ring}}^{1/7} m_{\text{ring}}^{6/7} t_{\text{Myr}}^{5/14} \mu_{q,10}^{15/8} \mu_b^{39/14}}{\eta_{0.1}^{31/28} R_{\text{in},15}^{155/56}}. \quad (16)$$

Figure 3 shows our model compared to the observed outburst decay flux for SGR 0418+5729 (Esposito et al. (2010)). The best fit is obtained for $\tau_d = 100$ days, $\mu_r = 8.1$ and a flux during quiescence of $F_{\text{HS,q}} \sim 10^{-13}$ erg cm^{-2} s^{-1} (i.e. $L_{\text{HS,q}} = 4.8 \times 10^{31}$ erg s^{-1} at 2 kpc).

In general it is hard to know the true quiescent level of many of these objects, since they are observed so rarely when not in outburst. Nevertheless, a minimum value for the flux in quiescence can be obtained in our model for the maximum $\mu_r = 28$ which corresponds to $\mu_q = 28$ (i.e. $N_e = 1$) and $\mu_b = 1$ (corresponding to a proton-rich atmosphere). The corresponding best fit (shown as dashed line in Figure 3) is obtained for $\tau_d = 160$ days and $F_{\text{HS,q}} = 2.5 \times 10^{-15}$ erg cm^{-2} s^{-1} . However this $\mu_r = 28$ fit misses the most recent measurements.

Our favored fit above with $\mu_r \sim 8.1$ (i.e. $\mu_q \sim 12.2$ for $\mu_b \sim 1.5$) implies an atmosphere temperature of ~ 6.3 eV (from $\mu \sim 6.1/T_{0.1}^{1/4}$ keV). Adopting the lower limit of 16 Myr for the age of the system ($P/3\dot{P}$), a self-consistent fit with $T_{\text{ring,q}} \sim 6.3$ eV (into eq. (3)), and $F_{\text{HS,q}} = 10^{-13}$ erg cm^{-2} s^{-1} (i.e. $L_{\text{HS,q}} \sim 4.8 \times 10^{31}$ erg s^{-1} into eq. (7)) is obtained for the following current ring properties

$$\begin{aligned} R_{\text{in}} &\sim 36 \text{ km} \\ R_{\text{out}} &\sim 56 \text{ km} \\ \Omega_{\text{ring}} &\sim 6.6 \times 10^{-3} \\ m_{\text{ring}} &\sim 2.5 \times 10^{-10} M_{\odot} \\ \rho_{\text{ring}} &\sim 2 \times 10^4 \text{ gm cm}^{-3}. \end{aligned} \quad (17)$$

The ring's mass was obtained by equating the observed burst energy of $\sim 6 \times 10^{37}$ erg into our eq. (12). The ring's atmosphere has a thickness of $H_{\text{atm.}} \sim 0.1$ cm and a mass of $m_{\text{atm.}} \sim 5 \times 10^{12}$ gm. The corresponding HS emitting area during quiescence (eq. 10) is $A_{\text{HS,q}} \sim 8 \times 10^7$ cm^2 . Also, eq. (10) gives $A_{\text{HS,q}}/A_{\text{HS,b}} = (\mu_b T_{\text{b,keV}}^{1/4})/(\mu_q T_{\text{q,keV}}^{1/4})$ which implies a HS emitting area during burst of $A_{\text{HS,b}} \sim 2 \times 10^8$ cm^2 . Finally, using the values above in eq. (16) we get $\tau_d \sim 0.4$ days $\mu_b^{39/14}$. Adopting an average μ during accretion of $\mu_{\text{b,av.}} \sim (\mu_q + \mu_b)/2 \sim 6.8$ gives $\tau_d \sim 91$ days which is close to the fit best fit value of 100 days.

⁴ For younger sources with $\Delta R_{\text{ring}} \sim R_{\text{in}}$, the ring's solid angle and area have different dependency on ring parameters which leads to $L_{\text{HS,b}} \propto (1/\mu)^6$ (eq. 28 in OLNII; see also Figure 2 in that paper) instead of the $L_{\text{HS,b}} \propto (1/\mu)^{39/14}$ for older sources as is the case here.

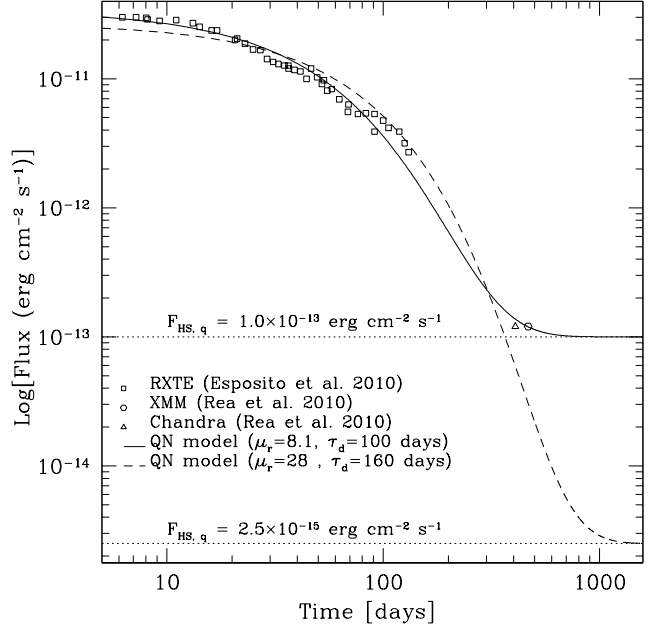


Figure 3. Outburst X-ray flux of SGR 0418+5729 as seen by RXTE, XMM and Chandra. Our model's best fit is obtained for $\tau_d = 100$ days, $\mu_r = 8.1$ and a quiescent flux $F_{\text{HS,q}} \sim 10^{-13}$ erg cm^{-2} s^{-1} (i.e. $L_{\text{HS,q}} \sim 4.8 \times 10^{31}$ erg s^{-1} for a source at 2kpc). Our model gives $L_{\text{HS,q}}/L_{\text{HS,b}} = 1/\mu_r^{39/14}$ at $t_b = 0$ (start of outburst; eq.(15)). The maximum value of $\mu_r = 28$ (see text) implies a minimum quiescent flux of $F_{\text{HS,q}} \sim 2.5 \times 10^{-15}$ erg cm^{-2} s^{-1} and requires $\tau_d = 160$ days for the best fit (dashed line).

4 PREDICTIONS AND CONCLUSION

1. SGR 0418+5729's current ring's mass is $\sim 2.5 \times 10^{-10} M_{\odot}$ extending from $R_{\text{in}} \sim 36$ km to $R_{\text{out}} \sim 56$ km (see 1). The ring's mass at birth is $m_{\text{ring}}^0 > 9 \times 10^{-7} M_{\odot}$ found from the $\tau_{\text{ring}} > t_{\text{age}}$ constraint. Given their degenerate nature the rings would have a very weak optical signature (unlike what would be expected from non-degenerate fall-back disks around neutron stars).
2. SGR 0418+5729's fit parameters give $m_w \sim 3 \times 10^{-16} M_{\odot}$. The wall is consumed on timescales given by eq.(22) in OLNII which yields a wall consumption time of < 1 hour for SGR 0418+5729.
3. Our model predicts a glitch, during the bursting phase (see eq.(29) in OLNII), of

$$\frac{\Delta P}{P} \sim -1.3 \times 10^{-10} \frac{P_{10} R_{\text{in},15}^{23/8} m_{\text{ring},-7}^{6/7} \mu_{q,3.3}^{15/8}}{I_{45} \eta_{0.1}^{5/4} t_{\text{Myr}}^{1/2}}, \quad (18)$$

where I_{45} is the star's moment of inertia in units of 10^{45} gm cm^2 . Using the best fit parameters for SGR 0418+5729 gives $\Delta P/P \sim -2 \times 10^{-11}$.

4. Fundamentally, the two-components model (QS and ring) provides a natural explanation for multiple emission components: vortex annihilation, the HS on the QS and the illuminated ring. However, as the system ages (i.e. at smaller \dot{P}), the ring becomes thinner in height and more extended in radial width and area. The feed-

back effect is reduced and so the ring's temperature decreases which makes the ring's contribution during quiescence harder to detect for old sources. In the case of SGR.0418+5729, and after full recovery from bursting phase, we predict a 2-component spectrum. The HS at ~ 0.67 keV and the ring at $T_{\text{ring}} \sim 6.3$ eV. A third, much weaker, component would be related to the emission from the magnetic field reconnection at the surface of the QS following vortex expulsion and annihilation. Assuming a BB emission, the temperature of the QS would be $T_{\text{QS}} \sim 17.3$ eV $\dot{P}_{-11}^{1/2}/R_{\text{QS},10}^{1/2}$ or < 0.4 eV in the case of SGR.0418+5729.

5. During the bursting phase the ring's atmosphere material (in particular protons and α particles) will emit a cyclotron line $2\pi\nu_p \sim eB_{\text{in}}/(m_Hc)$ with $B_{\text{in}} = B_s(R_{\text{QS}}/R_{\text{in}})^3$ and $B_s = \sqrt{3\kappa P\dot{P}} \sim 5.2 \times 10^{14} P_{10}^{1/2} \dot{P}_{-11}^{1/2}$. Recalling that a 1 keV line corresponds to 2.42×10^{17} Hz this gives $\nu_p \sim 1$ keV $P_{10}^{1/2} \dot{P}_{-11}^{1/2} R_{\text{in},15}^{-1/2}$. For SGR.0418+5729 we get $\nu_p \leq 0.05$ keV and $\nu_\alpha = 0.5\nu_p \leq 0.025$ keV.
6. During quiescence, the ring atmosphere (and thus the accreted material), is composed mostly of pure iron group nuclei. However, during the bursting phase and after irradiation, the atmosphere should be composed mostly of protons, of α particles and of ionized nuclei with $A \sim 28$ ($\mu = \mu_b \sim 1.5$). It would be interesting to look for such signatures in emission during quiescence and bursting episodes.
7. A key difference between objects showing magnetar-like activity and regular pulsars is the lack of persistent radio emission in the former class of objects. In our model the vortices force the interior magnetic field to align with the rotation axis, thus inhibiting persistent radio pulsation (Ouyed et al. (2004, 2006)). However, if SGR.0418+5729 has entered the last stages of ring consumption ($t_{\text{age}} \sim \tau_{\text{ring}}$), it should eventually show sporadic radio emission as it makes its way back to the vortex band as a RRAT (see OLNIII). This suggests that the system is in the last $\sim 1\%$ of its lifetime and currently descending from the accretion band back to the vortex band.

The above listed predictions in general produce weak signals: (i) Predictions 1&4 yield a flux of $\sim 10^{-19}$ ergs $\text{cm}^{-2} \text{s}^{-1} \text{\AA}^{-1}$ which corresponds to a 26-27 magnitude in the V-band at 2kpc. This is in principle detectable from eight meter class telescopes. The signal from vortex annihilation is much weaker; (ii) for prediction 2, the next burst is not expected until of order of 2000 years from now; (iii) for 3 the glitch is small compared to ordinary pulsar glitches (10^{-9} to 10^{-7}) requiring timing precision higher than possible for a transient source; (iv) for 5 the frequency is below the Lyman limit and the line would be absorbed by the hydrogen in the ISM; (v) for 6, the flux during outburst is high enough to check existing X-ray spectra for intermediate elements lines; for 7, unfortunately the timescale to evolve into a RRAT is of the order of 10^4 - 10^5 years. In summary, predictions 4 and 6 are the most testable.

ACKNOWLEDGMENTS

This research is supported by grants from the Natural Science and Engineering Research Council of Canada (NSERC).

REFERENCES

- Arnaud M., & Rothenflug R., 1985, A&AS, 60, 425
 Esposito, P. et al. 2010, MNRAS, 405, 1787
 Kaspi, V. M. 2010, Publ. of the Nat. Academy of Science, 107, 7147
 Göğüş, E., Woods, P. & Kouveliotou, C., Astron. Telegram, 2076 (2009).
 van der Horst, A. J. et al. 2010, ApJ., 711, L1
 Iwazaki, A. 2005, Phys. Rev. D, 72, 114003
 Kallman, T. R. & McCray, R. 1982, ApJS, 50, 263
 Keränen, P., Ouyed, R., & Jaikumar, P. 2005, ApJ, 618, 485
 Lyutikov, M. 2003, MNRAS, 346, 540
 Makishima, K. 1986, in LNP Vol. 266: The Physics of Accretion onto Compact Objects, ed. K. O. Mason, M. G. Watson, and N. E. White, 249
 Niebergal, B., Ouyed, R., & Leahy, D. 2006, ApJ, 646, L17
 Niebergal, B., Ouyed, R., Negreiros, R., & Weber, F. 2010a, Phys. Rev. D, 81, 043005
 Niebergal, B., Ouyed, R., & Jaikumar, P. 2010b, Phys. Rev. C. (Rapid Commun.), In Press [arXiv:1008.4806]
 Ouyed, R., Dey, J., & Dey, M. 2002, A&A, 390, L39
 Ouyed, R., Elgarøy, Ø., Dahle, H., & Keränen, P. 2004, A&A, 420, 1025
 Ouyed, R., Niebergal, B., Dobler, W., & Leahy, D. 2006, ApJ, 653, 558
 Ouyed, R., Leahy, D., & Niebergal, B. 2007a, A&A, 473, 357 [OLNI]
 Ouyed, R., Leahy, D., & Niebergal, B. 2007b, A&A, 475, 63 [OLNII]
 Ouyed, R., Leahy, D., Niebergal, B., & Yue, Y. 2009, MNRAS, 396, 1058 [OLNIII]
 Ouyed, R., Leahy, D., & Niebergal, B. 2010, A&A, 516, A88 [OLNIV]
 Rea, N., et al. 2010, Science, 330, 944
 Rengarajan, T. N. 1973, International Cosmic Ray Conference, 1, 627
 Thompson, C. & Duncan, R.C. 1995, MNRAS, 275, 255
 Trümper, J. E., Kylafis, N. D., Ertan, Ü., & Zezas, A. 2010, arXiv:1011.1678
 Vogt, C., Rapp, R., & Ouyed, R. 2004, Nuclear Physics A, 735, 543

This paper has been typeset from a \TeX / \LaTeX file prepared by the author.